

Static and kinematic testing of tiltmeters: facilities and results



Helmut Woschitz and Klaus Macheiner

Abstract

Today tiltmeters are widely used, often as part of measurement systems. In civil engineering applications, an accuracy of about 0.01° for the inclination is sufficient for many purposes. However, before using a specific type of sensor, it is most important to know about its performance, in static as well as in kinematic situations. But often, the required information is not provided by the manufacturer, and thus tests by the user are essential. We have developed testing facilities and a simple testing sequence for the determination of basic static and dynamic parameters of tiltmeters. The capability of the facilities is described in this article, and the results of the testing sequence are shown for one sensor exemplarily.

Kurzfassung

Neigungssensoren werden heutzutage vielfältig eingesetzt und sind oft Teil komplexer Messsysteme. Bei deren Einsatz im Bauwesen ist für die meisten Anwendungen eine Genauigkeit von ca. 0.01° ausreichend. Trotz dieser auf den ersten Blick nicht besonders herausfordernd erscheinenden Genauigkeit ist es notwendig, das Verhalten des Neigungssensors sowohl im statischen als auch im kinematischen Einsatz zu kennen, um diese Genauigkeit unter jeglichen Bedingungen einhalten zu können. Hersteller von Neigungssensoren stellen allerdings nicht immer oder nur teilweise Qualitätsinformation über ihr Produkt zur Verfügung. Daher sind Tests dringend notwendig. Wir stellen in diesem Beitrag Testeinrichtungen und –abläufe zur Untersuchung von Neigungssensoren vor, mit deren Hilfe einige grundlegende statische und dynamische Kenngrößen abgeleitet werden können. Die Möglichkeiten der Testeinrichtungen und die Ergebnisse für einen ausgewählten Sensor werden gezeigt.

1. Introduction

Today, tiltmeters are often part of measurement systems that are used in static and kinematic applications, see [1] to [4] for examples. In civil engineering applications, an accuracy of 0.001° is often sufficient for the inclination measurements. With this accuracy, a pre-fabricated component (that may be part of a larger structure) of 10 m in length, for example, may be aligned vertically within a tolerance of 10 mm. However, this tolerance must be preserved in static and kinematic conditions.

Usually, a tiltmeter is attached to the component and cannot be removed during its guiding process. Typical time spans for such a guiding process of a component are several hours up to a few weeks. Therefore, the long term performance, the zero point stability, the temperature dependence and the dynamic properties of a tiltmeter are of special interest. Not all manufacturers provide information about these parameters, and especially the specifications of low-cost sensors are often incomplete, see chapter 2 for example. Therefore, additional information about the sensor is necessary in order to guarantee the specified tolerance.

We have established a simple testing sequence (chapter 3) to acquire basic information about individual inclination sensors. Using this sequence, static and dynamic properties can be determined. In chapters 4 and 5, the static and kinematic testing facilities needed for testing are described. The testing sequence was applied to a sample of tiltmeters, and the results will be shown in chapter 6 exemplarily.

2. Tiltmeters

2.1. Tiltmeter samples

There is a variety of different tiltmeters available on the market. Within the last years, we have purchased several inclination sensors from different manufacturers with different operating principles, different precisions and various areas of application. Table 1 gives an overview about these sensors. In addition, the sensor's basic operating principle, as well as its output (analogue, digital), its working range (R), resolution (q), accuracy (a), linearity (l) and stability of zero offset ($\Delta\beta^0$) is listed. The listed information was extracted from manuals or other sources provided by the manufacturers.

Manufacturer	Model	Operating principle	A/D	$R[^\circ]$	$q[^\circ]$	$a[^\circ]$	$l[\%]$	$\Delta\beta^0[^\circ]$
AOSI	EZ-Tilt 5000-15 VIB	fluid / electrodes	A	15	0.004	—	< 0.3	—
Applied Geomechanics	Little Dipper Mod. 906	fluid / electrodes	A	10	0.005	—	0.8	—
Crossbow	CTXA02-T	seismic / capacitive	A	75	0.050	< 0.500	< 0.5	0.2
GeoKon	Model 6350	seismic / vibrating wire	D	10	0.003	0.02	0.3	—
HL-Planartechnik	NS-5/P2	fluid / electrodes	D	5	0.001	0.005	< 0.08	—
Interfels	EL 211.7115	fluid / electrodes	A	10	< 0.001	—	< 0.03	—
KELAG	SCA124T-D04FA	seismic / capacitive	A	90	0.003	—	—	< 0.03
MOBA	Dual Axis Slope Sensor	fluid / electrodes	D	60	0.010	—	0.03	0.1
Schaevitz	LSRP – 14.5	pendulum / servo	A	15	< 0.001	0.006	—	—
SEIKA	N3	fluid / capacitive	A	30	0.005	—	< 0.2	—
Wyler	Zerotronic Type 3-10	pendulum / capacitive	D	10	< 0.001	—	< 0.001	—

Table 1: Sample of tiltmeters and basic specifications

The listed specifications differ widely, and sometimes there is even no information available for a specific property (indicated by “—”).

The choice of tiltmeters was based on recommendations given in the literature or personally by other users. Actually, the sample does not include sensors with automatic reversal measurement, mainly because of their high costs.

2.2. Preparation of the sensors

The base plate of some sensors is not adequate for the precise determination of zero offsets (e.g., bad quality in flatness). Therefore, each sensor was attached to a separate base plate that provides three-point bearing and therefore allows the reproducible set up of the sensor.

For the digital sensors, specific data acquisition software had to be programmed to get at least data rates of 10 Hz with a standard PC. Data conversion from raw (e.g., [V], [mA]) to angular units [°] is also performed by these routines. New calibration parameters had to be determined for the sensors, where no or inaccurate parameters were provided by the manufacturer.

3. Testing sequence

For modern instruments, often little information about the operating principle, the setup or the calibration functions applied by the manufacturer is available. Then, the sensor may be considered as a general measurement system that transforms an input signal $x(t)$ into an output signal $y(t)$, e.g. [5].

In the case of a tiltmeter, $x(t)$ will be the inclination applied to the object carrying the sensor. The output $y(t)$ is dependent on the characteristics of the individual components of the sensor. Additionally, the output may be affected by external disturbances. Such disturbances may be caused by vibrations or changing temperatures for example.

There are two simple possibilities to obtain information about the measurement system. The output $y(t)$ is investigated, (a) while external disturbances are applied to the system and the input $x(t)$ is kept constant, or (b) while the input $x(t)$ is changed and no disturbances are present. Both are used in the test sequence described in the following.

A commonly known error source in inclination measurements is the zero offset β^0 , which can be determined easily by reversal measurement, [6]. Changing conditions may cause changes of β^0 . This is why the repeated determination of β^0 is a central part of the testing sequence. Additionally, tests on the sensor's self-heating and temperature dependence as well as kinematic tests are performed. An outline overview of the testing procedure is given in table 2.

Tests A and B should show the performance of a sensor when self-heating. The fully acclimatised sensors were switched on immediately before starting the measurement. Tests C followed in order to determine β^0 for the sensors at working temperature. For the investigation of the acclimatisation performance (tests D and F), the sensor was heated up to +40°C and cooled down to –10°C in a climatic chamber, respectively

(storage period in the chamber at least 7 hours). Afterwards, they were put to a granite plate (fig. 1), and data acquisition started. In order to avoid effects due to self-heating, all sensors were switched on in the climatic chamber and data output was active. Again, the determination of β^0 followed tests D and F. In order to investigate the stability of β^0 whilst the kinematic tests (test I), β^0 was determined before and after this test, too.

#	Name of the test	duration
A	determination of β^0	1 h
B	self-heating performance	> 36 h
C	determination of β^0	1 h
D	acclimatisation(temperature change: +40°C → +20°C)	> 36 h
E	determination of β^0	1 h
F	acclimatisation(temperature change: -10°C → +20°C)	> 36 h
G	determination of β^0	1 h
H	determination of β^0	1 h
I	kinematic test (3 runs)	0.5 h
J	determination of β^0	1 h

Table 2: Overview of the test cycle

Reversal measurements were used to determine β^0 , where data were sampled for 60 seconds in each position. Prior to data acquisition, a waiting period of 60 seconds was used in order to avoid settling errors. The determination of β^0 was repeated 10 times in every test to check the repeatability.

For all static experiments (A-H, J), the sampling period was set to 10 Hz. This is considered to be a good compromise, when considering the need of many kinematic applications. However, some digital sensors provide lower sampling rates.

The duration of tests B, D and F was longer than 36 hours in order to be able to detect drifts after the acclimatisation period in the beginning.

For practical reasons, the static tests were carried out simultaneously for several sensors (in our case four). Contrary, the kinematic tests were done individually, as the kinematic test facility (see chapter 4) can carry only one sensor. Moreover, the sampling frequency was higher in the case of kinematic testing (9600 Hz for analogue sensors, maximum sampling frequency possible for digital sensors), based on the idea to determine natural frequencies.

If a project gets to a well defined stage and more information about the site conditions

become available, a more intensive investigation of appropriate sensors should be carried out. At least, the whole test cycle should be repeated for the sensors under consideration.

4. Static test facility

The performance of tiltmeters might depend on various factors (e.g., temperature, mechanical stress). When testing an instrument, only one of these factors should be varied to get the system's response for one single dependency. Testing is done best in a laboratory with constant temperature and a stable foundation. The geodetic laboratory of the institute (approx. 33 × 6.5 m² in size) is climatically controlled (temperature: 22.0°C ± 0.5°C, humidity: 50% ± 10%) and set up on a stable base.

For the tests described above, a stable base plate is needed in order to allow the reproducible set up of the sensors. For that purpose we use a plane granite plate which is set up in the laboratory. Figure 1 shows this plate with the required mounting accessories and four sensors under test.

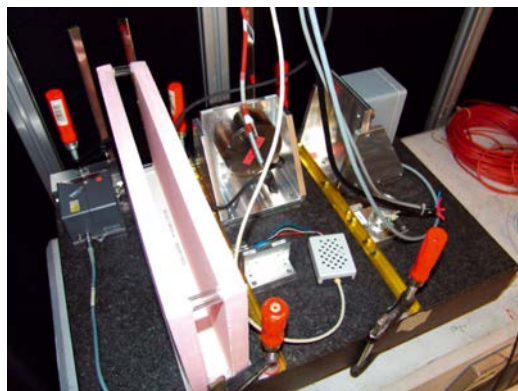


Figure 1: Granite plate with mounting accessories and sensors under test

The stability of the granite plate is continuously monitored by a Leica Nivel20 inclination sensor, which is known to be highly precise under stable thermal conditions. Figure 2 shows the result of this continuous monitoring during a time period of two years.

A heat radiation shield (pink Styrofoam plates in fig. 1) was used for not disturbing the Nivel20 during the acclimatisation experiments. However, it was still slightly disturbed (outliers indicated by red dots in fig. 2).

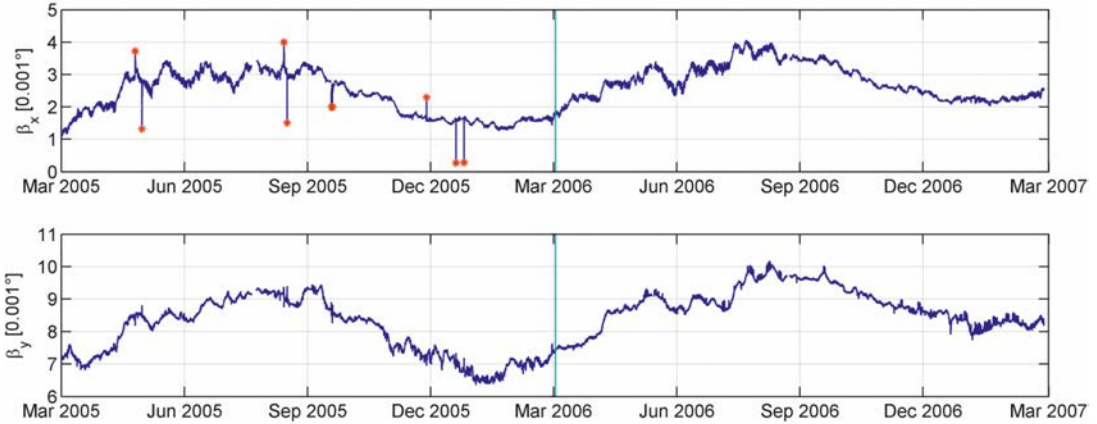


Figure 2: Biaxial Stability of the granite plate monitored by a Leica Nivel20.

An annual cycle is apparent for both axes, where the inclinations change for about 0.003°. Thus, the stability of the granite plate is sufficient for the static tests, which do not last longer than two days.

The laboratory also houses a climatic chamber (volume 1 m³, temperature range: -10°C to +40°C), which was used to expose the sensors to different temperatures prior to the acclimatisation experiments.

5. Kinematic test facility
5.1. Testing functions

The performance of measurement systems may be investigated using testing functions, see [5] for example. The response $y(t)$ of a system is investigated by changing the input $x(t)$ according to a known testing function. The kinematic test facility described later was constructed in order to generate a testing function $f_P(t)$, consisting of a ramp, $f_R(t)$, and a step function, $f_S(t)$, as shown in fig. 3.

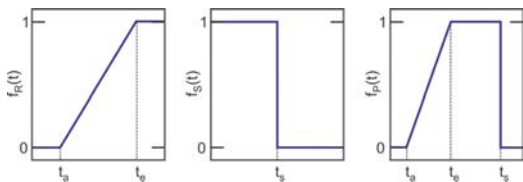


Figure 3: Ramp (left), step (middle) and composed testing function (right).

A tiltmeter represents a measurement system of second order, for example see [6] or [7]. Applying the testing function $f_P(t)$ to the system

and investigating the system response, typical parameters like the natural frequency f and the damping coefficient δ may be determined (for details see [8]).

5.2. Design and experimental set up

A specific test facility is needed in order to apply the testing function $f_P(t)$ (fig. 3, right) to the sensor under test. Its principle is illustrated in fig. 4.

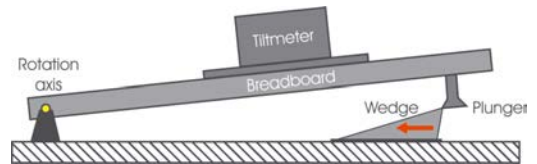


Figure 4: Principle of the kinematic test facility.

The tiltmeter is attached to a breadboard, which may be rotated about a horizontal axis. The rotation is induced by a horizontally moving wedge (1 mm/s) that is attached to a translation stage and lifts up a plunger, which is fixed to the bottom of the breadboard. The amount of the inclination change (ramp function) is about 0.45°. After the plunger has reached the upper end of the wedge, the breadboard suddenly returns to its initial horizontal position and thus realizes the step function. The height of the fall does not exceed 2 mm, in order to avoid damaging the sensor by the shock induced by the impact. The time of the impact and its load after the fall are determined by using accelerometers mounted additionally at the breadboard (fig. 5). During the experiments, impact loads of up to 40 g were measured.

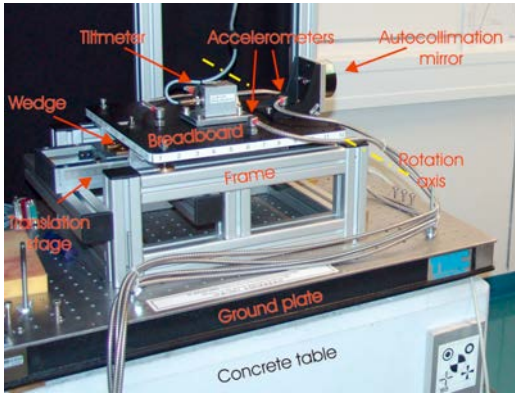


Figure 5: Kinematic test facility with attached tiltmeter and accelerometers.

The kinematic test facility is set up in the laboratory of the institute on the same concrete table as the granite plate (see chapter 4). Using this facility, characteristic parameters like the natural frequency, the damping coefficient or the decay time may be determined for each individual sensor.

Three PCs and a data logger are used to operate the test facility. Time synchronization between the PCs is done using a synchronisation signal recorded simultaneously by all PCs (for details see [8]). In order to determine the time and load of the impact precisely, a sampling frequency of 9600 Hz was used.

For the analysis of the inclination data, reference values for the testing function realized by the testing facility are necessary (comparison of sensor output with reference values). These values were determined using a highly precise sensor (Wyler ZeroTronic). In order to keep dynamic influences as low as possible, the velocity of the translation stage was rather slow (0.1 mm/s) in this case. These values were controlled at 45 discrete points using autocollimation with a Wild T2000 theodolite. Differences between the two methods did not exceed 0.001° , which is sufficient for our investigations ($\sigma < 0.01^\circ$).

6. Analysis and results

All sensors listed in table 1 were tested in the same way, using the test sequence described in chapter 3. Here, the results of one sensor (Kelag SCA124T – D04FA, referred as KE in the following) are shown exemplarily. More details and further results are provided in [8] and [9].

6.1. Temperature experiments

Data were acquired with 10 Hz in order to get similar heating-up effects of the sensor as they might occur in field use. Before further processing, data of consecutive 10 second intervals were averaged in order to reduce data. This is applicable for the static tests, where inclinations change slowly.

Figure 6 shows the inclinations β measured with sensor KE for test B and F (see table 2) exemplarily. The values shown are already reduced for β^0 (determined by test C and G, respectively). Thus, the data at the end of the plots represent the true inclination of the granite plate, which was independently determined with the Nivel20 as -0.009° .

During both tests, the stability of the granite plate was better than 0.001° . Thus, values differing from -0.009° are originated by the self-heating and the acclimatisation of the sensor. In the beginning of the time series conditions change rapidly and strong variations can be seen. These variations are much larger than the resolution of the sensor (see table 1). Non-linear drifts as well as sudden inclination changes or even peaks are visible. These effects may be caused by the sudden expansion of individual parts of the sensor. As such effects are hardly reproducible and thus cannot be modelled, the range (rg) covered by the changes is numerically given in fig. 6 as one indicator. The end of this initial phase ($EoIF$) is indicated by a dashed vertical (red) line. After $EoIF$, the conditions are stable and the output values should remain constant. But even then, small linear drifts are present.

The position $EoIF$ is determined by means of linear regression analysis. This was favoured over e.g., modelling a measurement system of first order, because some sensors (so does the KE) correct the measured values by means of internal temperature measurements, so the remaining effects may differ significantly from a modelled system. Computation is done using outlier detection in order to find the section in the beginning of the time series. The a-priori variances σ^2 needed for the model test were determined for each sensor empirically, using a linear sample of the data set. In the case the empirical variance gets zero (i.e., for sensors with low noise and a large resolution), the variance of quantisation noise ($\sigma^2 = \frac{q^2}{12}$, see [10], pp.193) is used instead.

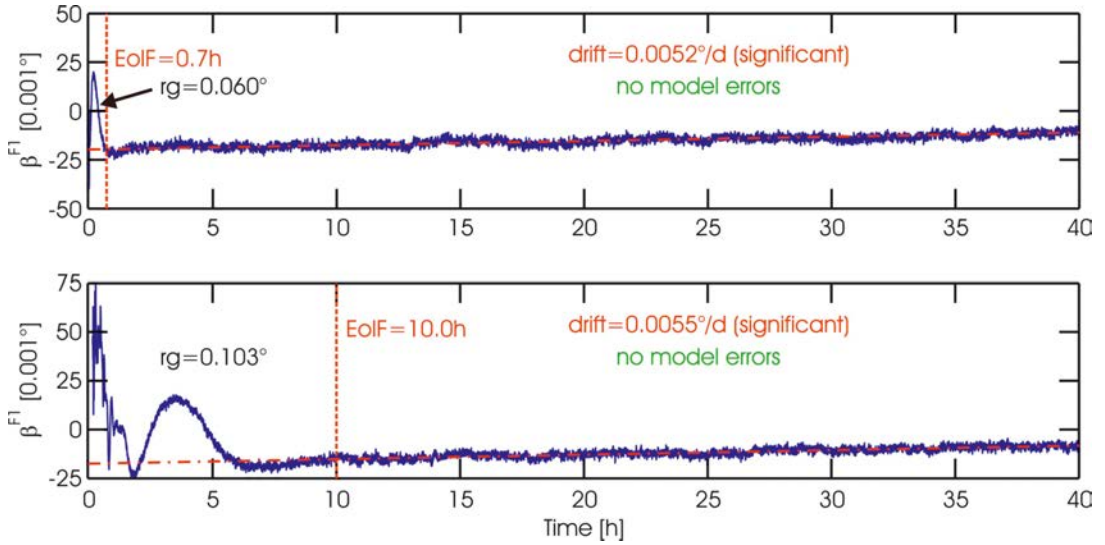


Figure 6: Inclination changes of sensor KE, caused by self-heating (test B, upper) and acclimatisation from -10°C to $+20^{\circ}\text{C}$ (test F, lower).

The slope of the regression line is an indicator for the drift of the sensor. It is determined by the data after $EoIF$ only. A numerical value is given for the drift, if the slope significantly deviates from zero (confidence level 99.7%) and its magnitude is larger than a threshold. There, the threshold is set by practical considerations, e.g., 0.002° per day if the sensor is used five days continuously in the guiding process of an object and the effect of the drift should remain smaller than 0.01° within that time.

6.2. Kinematic results

The difference ($\Delta\beta$) between the reference values of the kinematic test facility and the output of the sensor is shown in the upper part of fig. 7. The blue line represents the originally sampled data (9600 Hz, see section 5.2), and the yellow line shows a moving average (10 Hz, which may be a proper sampling frequency for various applications). Caused by the testing function $f_P(t)$, fig. 7 exhibits four parts: a region before the ramp (a), a section during the slope of the ramp (b), a part after the ramp (c) and an area after the step (d), see lower part of fig. 7.

Regarding the sections (a) and (d), where no inclination changes occur, robust means (m) and standard deviations (s) were calculated. The median absolute deviation (MAD, [11]) was used for that purpose. The means m and the confidence intervals (95 %) are depicted by red

and green lines, respectively. For the case of this sensor, there is no significant shift (Δm) in the robust means before (a) and after the impact (d).

The following sensor properties may be obtained by investigating the sensor’s behaviour in sections (a) to (d) of fig. 7:

- In the case of an ideal sensor, $\Delta\beta$ equals zero all the time, i.e. reference values and sensor output are identical.
- A shift in the robust means of section (a) and (d) would indicate a change of the zero point β^0 due to the impact. In both sections, the sensor’s output should hold a constant level, since no inclination changes take place.
- A delayed response of the sensor causes an offset in the ramp section (b).
- If a slope appears in the ramp section (b), data of the sensor may be affected by a “scale factor”. However, this is only representative for the small range of the test facility (0 to 0.45°) and may rather be caused by the calibration function used by the sensor. If needed, the scale factor over the whole working range of the sensor must be determined separately.
- After the ramp, section (c), the values for $\Delta\beta$ should return to the zero line. A remaining offset would be the consequence of the aforementioned “scale factor”.

The section of the step response is shown in fig. 8 in detail. This illustration corresponds to the end of

section (c) and the beginning of section (d) in fig. 7. The time stamp of the impact (dashed vertical line) is determined by the signal of the accelerometers.

The step response of sensor KE exhibits the behaviour of a measurement system of second order (section 5.1), with an additional exponential term. The eigenfrequency f was determined as $f = 75$ Hz. After the impact, the signal oscillates with an initial range (rg) of 9.7° . To characterize the decay behaviour, three thresholds were defined: (i) The value t_1 corresponds to the time after which a band of $\pm 5\%$ of the maximum amplitude is not exceeded any more [5]. (ii) Time t_2 indicates when the signal stays within a confidence level of 95%.

(iii) The threshold t_3 marks the time stamp when the oscillation is below 0.01° , which was the aim of the investigations. Figure 8 shows that the inclination signal does not exceed the 5% bounds after $t_1 = 0.05$ s and the confidence bounds after $t_2 = 0.10$ s. Decay time t_3 could not be computed in this case (precision of the signal approx. 0.035°). The short decay times indicate the strong damping of the sensor ($\delta > 100$). At a practically acceptable sampling rate of 10 Hz, for example, the magnitude of the impact's reaction decreases dramatically down to 0.12° due to averaging effects. More details and results of other sensors are given in [8].

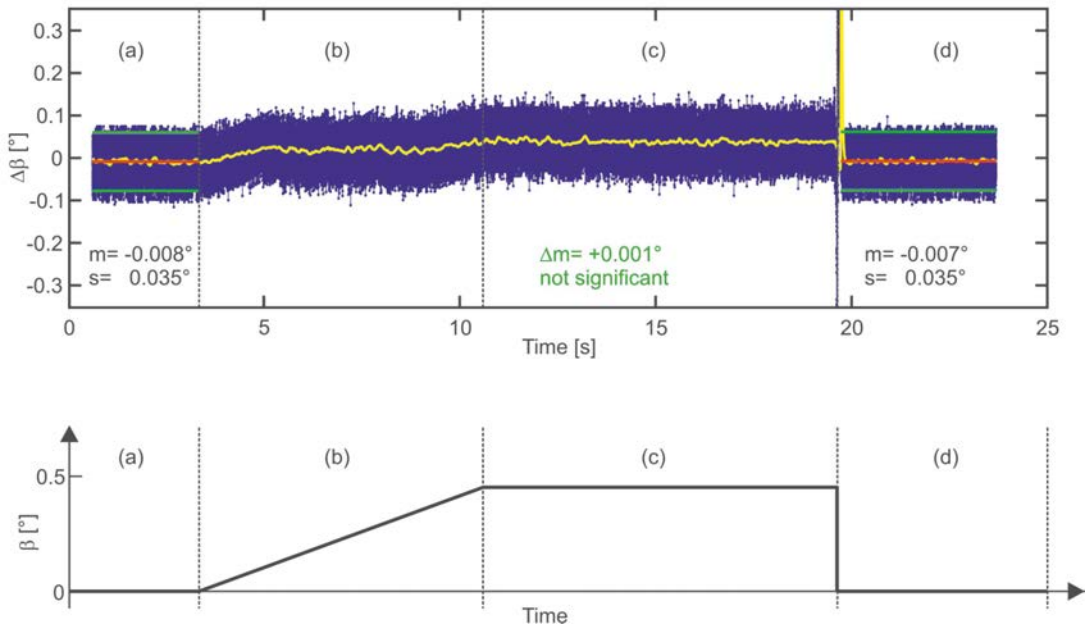


Figure 7: Difference between the reference values of the kinematic test facility and the sensor's output (upper) and the related sections of the testing function (lower).

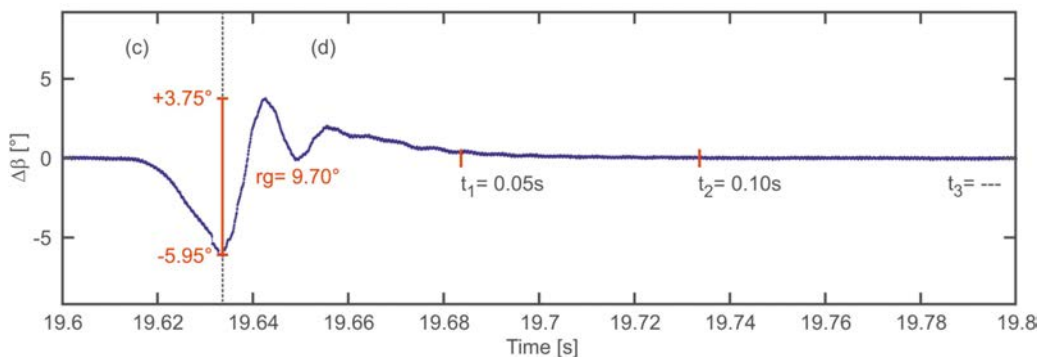


Figure 8: Step response of sensor KE.

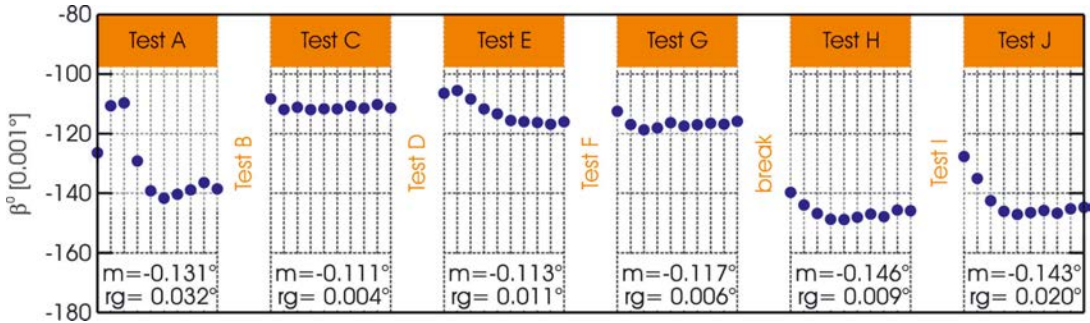


Figure 9: Zero points of the sensor KE.

6.3. Stability of zero points

In the case of the reversal measurements for the zero points (60 sec data with 10 Hz), data evaluation is quite simple. After robust outlier detection, the remaining values are averaged to give one inclination value per set-up (β^{F1} , β^{F2}). Using these values, the zero point β^0 can be easily computed as well as the inclination β of the surface (granite plate):

$$\beta^0 = \frac{\beta^{F1} + \beta^{F2}}{2}, \quad \beta = \frac{\beta^{F1} - \beta^{F2}}{2} \quad (1)$$

The resulting zero points for the different experiments are shown in fig. 9 for the sensor KE.

For the assignment of the different tests, table 2 may be used. During each test, β^0 was determined 10 times and each individual β^0 is shown as a blue point. The mean value (m) and the range (rg) of the zero points are given numerically.

Sensor KE shows some variations of β^0 in the beginning of experiment A, which are caused by the self-heating of the sensor. The magnitude is comparable with the changes determined by test B in the initial phase (see fig. 6, upper plot). For the sensor at operating temperature (test C), only little variation is present. The values for β^0 determined immediately after the acclimatisation experiments (tests E and G) show a drift, which may be caused by a release of tensions during reversing the sensor. Tests H and J were carried out a few months later (after the establishment of the kinematic test facility), which may be responsible for the offset of β^0 determined within these tests. However, the observed variations of β^0 are within the range of the stability given by the manufacturer (0.03°). More details are given in [9].

7. Resume

There are large differences in the specifications of commercially available tiltmeters. The lack of some specifications, crucial for certain applications, can only be overcome by individual testing. We have presented some test facilities and a procedure which allow the determination of some basic static and dynamic properties of tiltmeters. The derived static parameters include zero point stability, self-heating effects, temperature dependencies and long term stability. The dynamic parameters comprise natural frequencies, damping characteristics and decay times.

The derived information is the same for all sensors under test, thus allowing a comparison of different sensors, which cannot be done easily using the varying information provided by the manufacturers. Of course additional investigations (e.g., linearity over the whole working range) have to follow, if the sensor was selected for a specific application. However, the presented facilities and procedures may be used to exclude sensors not fulfilling the defined criteria.

The shown sensor KE shows a desirable performance within the static and kinematic tests. The results do not disagree with the manufacturer's specifications. Although the specified stability of the sensor (0.03°) is little worse than our aspired 0.01° , the performance of KE is sufficient for many civil engineering applications.

Acknowledgements

R. Presl was responsible for setting up the test facilities and for programming the data acquisition software. He also carried out many experiments, assisted by R. Lummerstorfer. We are grateful for their various contributions to these investigations.

R. Ruland, Stanford Linear Accelerator Center, Stanford University, and A. Bühlmann, Leica Geosystems AG, provided several tiltmeters. Their cooperation and interest in our investigations are gratefully appreciated.

References

- [1] *R. Glaus, N. Lauener, U. Müller and M. Baumeler (2004):* Der Gleismesswagen swiss trolley: Leistungsmerkmale und Anwendungen. In: Ingenieurvermessung 2004 pp. 27-37. 14th International Course on Engineering Surveying. Zürich, March 15-19, 2004
- [2] *W. Stempfhuber (2006):* 1D and 3D Systems in Machine Automation. In: Proceedings of the 3rd IAG / 12th FIG Symposium, Baden. May 22-24, 2006
- [3] *H. Ingensand (1985):* Ein Beitrag zur Entwicklung und Untersuchung hochgenauer elektronischer Neigungsmesssysteme für kontinuierliche Messungen. Series C, Book No. 308, Bavarian Academy of Sciences, Munich
- [4] *E. Grillmayer, A. Wieser and F. K. Brunner (2000):* Einrichtung der Stahlpylone der Donaubrücke bei Pöchlarn. In: Ingenieurvermessung 2000 pp. 63-74. 13th International Course on Engineering Surveying. Munich, March 13-17, 2000
- [5] *P. Profos and T. Pfeifer (2001):* Grundlagen der Messtechnik. Fifth Edition. Oldenbourg, Munich
- [6] *W. Schwarz (1995):* Vermessungsverfahren im Maschinen- und Anlagenbau. Wittwer, Stuttgart
- [7] *D. Gross, W. Hauger, W. Schnell and J. Schröder (2004):* Technische Mechanik 3. Kinetik. Eighth Edition. Springer, Berlin
- [8] *K. Macheiner, H. Woschitz and F. K. Brunner (2007):* Test von dynamischen Eigenschaften ausgewählter Neigungssensoren. (Submitted for publication)
- [9] *H. Woschitz (2007):* Statische Eigenschaften ausgewählter Neigungssensoren. (Submitted for publication)
- [10] *A. V. Oppenheim and R. W. Schaffer (1999):* Discrete-Time Signal Processing. Second Edition. Prentice-Hall, Upper Saddle River (NJ)
- [11] *L. Sachs (1997):* Angewandte Statistik. Anwendung statistischer Methoden. Eighth Edition. Springer, Berlin

Contact

Dr. Helmut Woschitz: Engineering Geodesy and Measurement Systems, Graz University of Technology, Steyrergasse 30, 8010 Graz, Austria. E-mail: helmut.woschitz@tugraz.at
Dipl.-Ing. Klaus Macheiner: Engineering Geodesy and Measurement Systems, Graz University of Technology, Steyrergasse 30, 8010 Graz, Austria. E-mail: klaus.macheiner@tugraz.at 